Electrodeposition of polyaniline on acidified clay montmorillonite modified electrode

Duke Orata*, Fred Segor

Department of Chemistry, University of Nairobi, P.O. Box 30197, Nairobi, Kenya

Abstract

In this paper, we have presented results obtained on derivatization of the working electrode surface with clay montmorillonites treated with varying amounts of acid. The resultant changes in the population of Bronsted and Lewis acid sites is shown to affect the redox properties of conducting polymer, polyaniline. © 2000 Elsevier Science B.V. All rights reserved.

1. Introduction

Polyaniline is among the most studied of the conducting polymers. This stems from the fact that it is easy to synthesize, has a well behaved electrochemistry and is stable under ambient conditions [1–8]. These qualities are negated by the fact that at very high potentials, polyaniline degrades forming quinone/imine derivatives. Practical applications of polyaniline is also hampered by its poor processability.

Thus, our choice of a clay montmorillonite as our surface modification material was based on the realization that, in addition to the fact that, clay minerals are cheap, and have well-defined layered structures, flexible adsorption properties, higher thermal and chemical stability and potential as catalysts and/or catalyst support, the films used in our analysis unlike in the cases

reported previously [9–20] of thin films developed from spin-coating methods can be peeled off the electrode surface and subjected to further analysis.

Our objective was to further verify the effect on polyaniline redox chemistry of the population of Bronsted and Lewis acid sites on the clay montmorillonite, as previous work has shown that polyaniline redox properties are strongly pH dependent.

The next stage in this study involved electrodeposition of a conducting polymer on both raw and acid activated clay modified electrode to determine whether the cyclic voltammetric response of polymer is altered by the acidification process. The conducting polymer of interest here is polyaniline, a polymer synthesized by chemical oxidation of aniline in aqueous media. Alternatively like in our case, its films are routinely electrodeposited by potential cycling in acid solution containing aniline. Cycling to

*Corresponding author.

very positive potentials is normally avoided to deter the formation of quinone derivative [2]. The cyclic voltammogram of polyaniline shows a redox process at approximately 0.2 V with a relatively sharp peak for oxidation and a broad peak for the reduction.

2. Experimental

2.1. Chemical reagents

NaOH (Kobian), sulphuric and hydrochloric acids (Aldrich), pyridine (BDH) and cyclohexylamine (BDH) were used as received without further purification. Aniline (Aldrich) was triply distilled until a colourless liquid was obtained and was then stored under nitrogen. All the solutions were prepared using triply distilled water. The clay montmorillonite (bentonite, Athi River Mining Company, Kenya) was purified as described in references [21–23]. The latter has a mesh size ranging from 150 to 200 μm, cation-exchange capacity (CEC) 1.18–1.22 eq./g and a pH range of 8.4–9.6.

2.2. Electrochemical equipment/system

The electrochemical system comprised of a three-electrode assembly. Saturated calomel electrode (SCE), platinum wire and carbon graphite (bare surface area 0.38 cm^2) served as reference, auxiliary/counter and working electrodes, respectively. The cyclic voltammograms were generated using the PAR 175 universal programmer in conjunction with PAR 173 potentiostat/galvanostat. The output signal was fed into a X–Y recorder PAR RE 0089. The working electrode was polished using alumina on a felt polishing cloth for each fresh experiment.

2.3. X-ray fluorescence analysis

For X-ray fluorescence analysis, a Canberra Si (Li) detector system series 7300, detector

Table 1
Elemental composition of raw and acidified clay

Element	Concentration ($\times 10^{-3}$ g/g)			
	Raw	A1	A2	A3
K	8.35	2.69	4.145	6.31
Ca	37	34.6	33.65	32.95
Mn	0.581	0.026	0.0322	0.0188
Fe	50.5	38.7	20.7	9.91
Ni	–	0.00476	0.0051	0.00644
Cu	0.069	0.0312	0.0258	0.01063
Zn	0.096	0.0708	0.051	0.0296

model SL 30180 was used to determine the elemental composition of raw and acid activated bentonite. Pellet formation procedure was adopted for the sample preparation.

2.4. Infrared analysis

Pyridine adsorbed on Lewis and Bronsted sites of montmorillonite were determined by mixing separately 2 g of raw and acid activated bentonite with 3 ml of pyridine. The paste-like mixture/slurry was then ground uniformly and the acidity of the active sites in the solid samples monitored by SP3 300 infrared spectrophotometer. The same procedure was adopted in the case of cyclohexylamine [24].

2.5. pH analysis

Determination of the CEC, adsorbed and exchanged protons on bentonite was done using a Pye Unicam model 292 MK2 pH meter.

3. Results and discussion

3.1. Preparation of acidified bentonite for electrode surface modification

Several samples of acidified bentonite were prepared by mixing the clay with sulphuric acid at a pre-determined acid-to-clay (w/w) ratios i.e., sample A1 (0.35), sample A2 (0.60), sample A3 (0.90) and sample A4 (1.25). The resulting slurry from the mixture was dried at 95°C for 24 h. After drying the slurry was

washed with hot distilled water and the solid residue dried at 90°C for 24 h. The samples A1, A2 and A3 were used for electrode modification and were also subjected to IR and XRF analysis.

The elemental analysis data obtained for the samples are shown in Table 1.

The data obtained in Table 1, suggest that in all the cases the metal extraction increased with
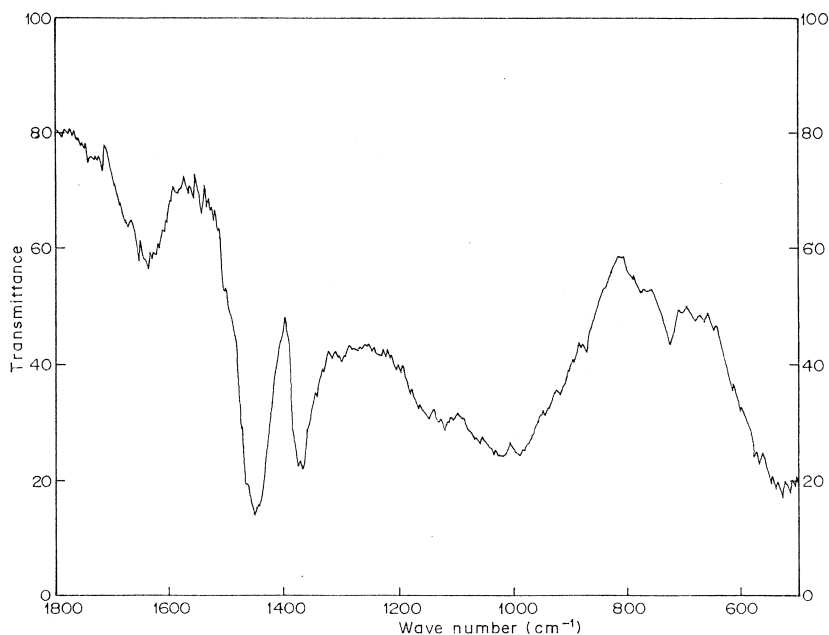

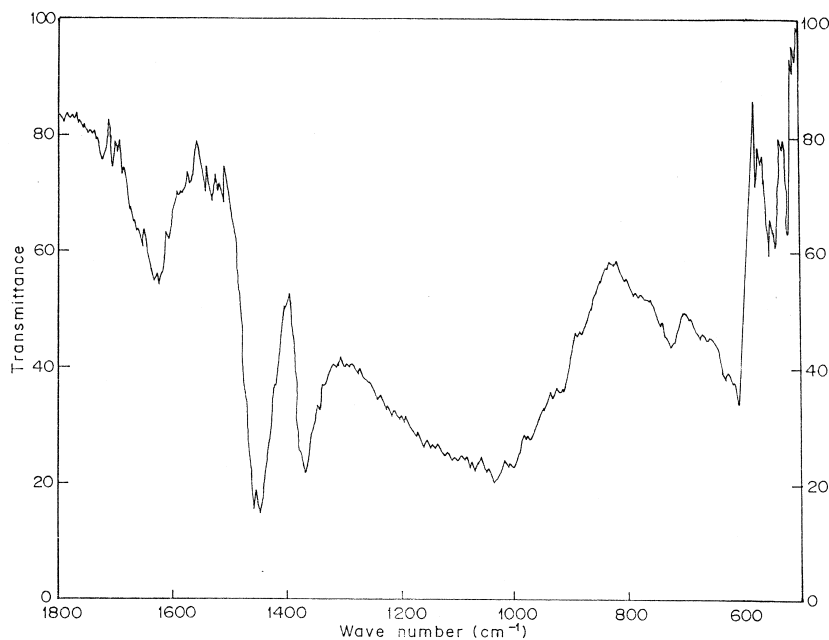Fig. 1. IR spectra of pyridine adsorbed in bentonite (standard).

Fig. 2. IR spectra of pyridine adsorbed in acid activated A1 sample.

the acid-to-clay ratio. When one considers the extraction of Ca cations, bearing in mind that they occupy the interlayer region of the clay, we observe that only 6% was extracted for the case of A1. Not much of a substantial drop was recorded at the higher acid-to-clay ratios. The poor extraction of calcium can be attributed to the Ca^{2+} ions binding partially on the degraded montmorillonite. Fijal et al. [25] attributed this to the attachment of Ca^{2+} ions to centres of
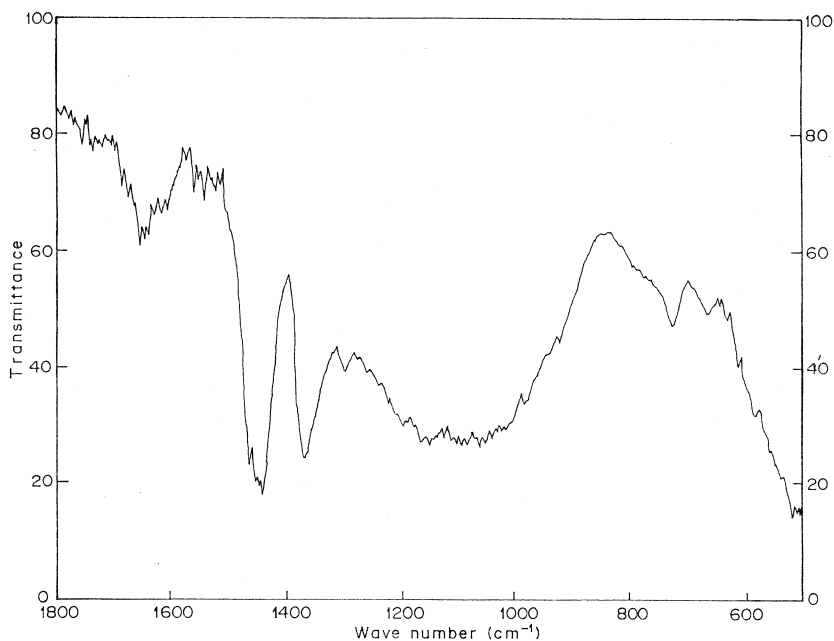

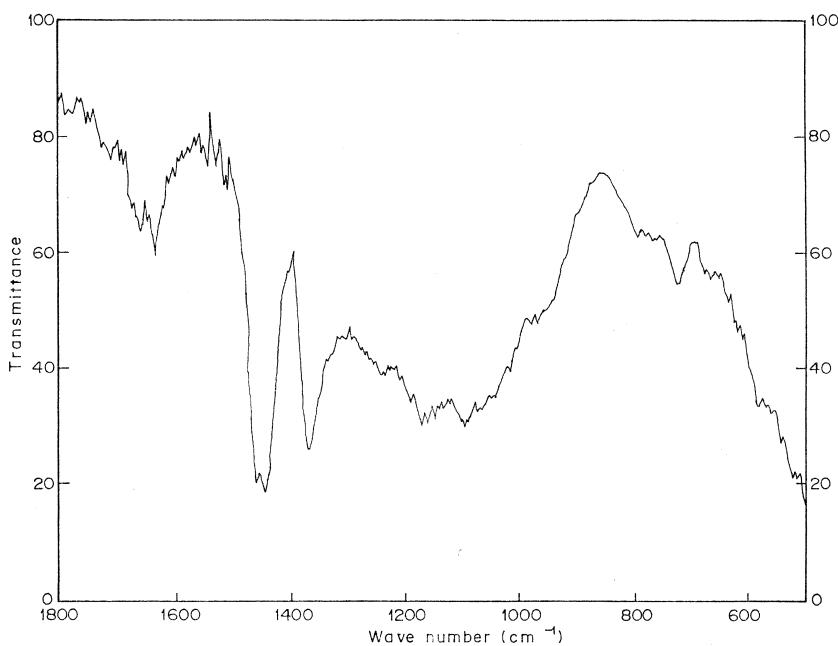Fig. 3. IR spectra of pyridine adsorbed in acid activated A2 sample.

Fig. 4. IR spectra of pyridine adsorbed in acid activated A3 sample.

negative charge found in certain regions of the tetrahedral layers and thus, capable of bonding strongly with the Ca^{2+} ions. The metal extraction pattern for Fe, an octahedral ion, is quite different from that of calcium. This is expected as Fe and Ca ions do not occupy identical positions in the clay. The extraction pattern of monovalent ions i.e., K was also observed to be quite different from that of multiply charged ions as expected since they do not occupy the same sites.

In general it appears that at an acid-to-clay ratio of 0.35, the ease of removal of the ions follow the order $Ca > K > Cu > Mn > Fe$. This relationship is probably attributed to the fact that the extraction of the metal ion depends on the cation–oxygen bond. Thus, Fe which has the highest ionic potential is the most difficult to extract.

3.2. Infrared spectroscopic analysis of acidified bentonite

The Lewis and Bronsted acid sites on the raw bentonite and acidified bentonite samples were identified from the IR spectra of pyridine on these samples. The spectra obtained are shown in Figs. 1–5. In general, pyridine adsorbed on a Lewis acid site will adsorb at ≈ 1450 and 1620 cm^{-1}, whilst that adsorbed on a Bronsted acid site will adsorb at ≈ 1540 cm^{-1}. A band at ≈ 1490 cm^{-1} suggests pyridine on both Lewis and Bronsted acid sites [24].

It is apparent that the acidified bentonite samples A1, A2, A3 and A4 have a higher proportion of Bronsted acid sites, while the raw bentonite has a higher proportion of Lewis acid sites. This is in agreement with observations by other workers [24] since during the metal extraction from tetrahedral layer, we are reducing the number of acid sites capable of undergoing isomorphous substitution i.e. Fe^{3+} for Si^{4+} in the tetrahedral layer. This action does not lead to any increment in the Bronsted acidity. The latter is affected on acidifying the montmorillonite since acidification leads to the presence of protons on the matrix, thus increased Bronsted acidity.

Acidified bentonite has fewer isomorphously substituted M^{3+} (where M represents metal cations such as Al, Fe, etc) as compared to raw bentonite. It is also important to mention that, in
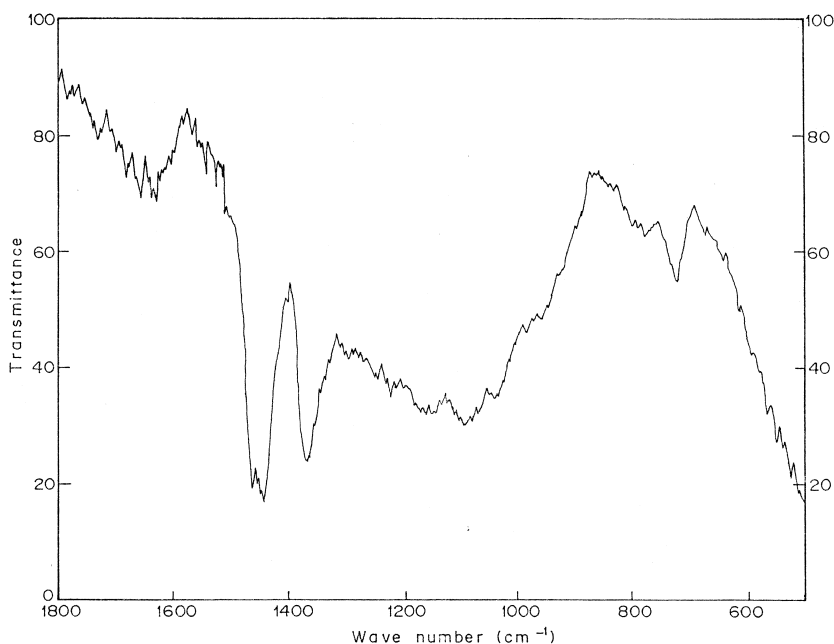

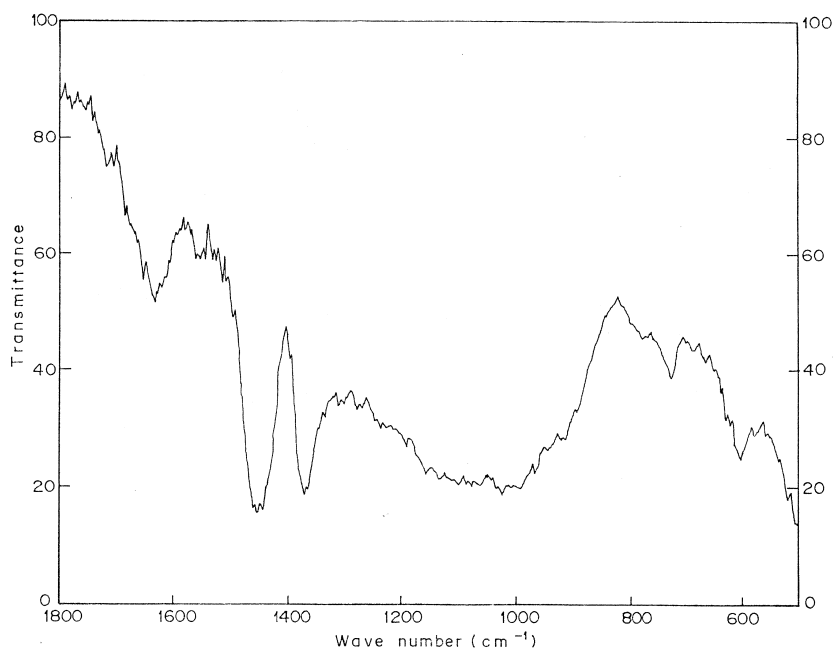Fig. 5. IR spectra of pyridine adsorbed in acid activated A4 sample.

Fig. 6. IR spectra of cyclohexylamine adsorbed in acid activated A1 sample.
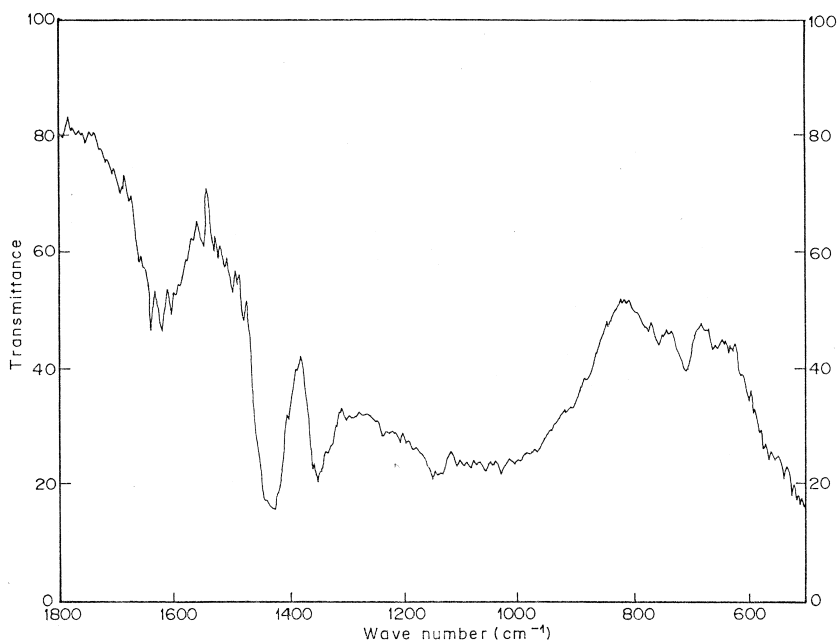

Fig. 7. IR spectra of cyclohexylamine adsorbed in acid activated A2 sample.
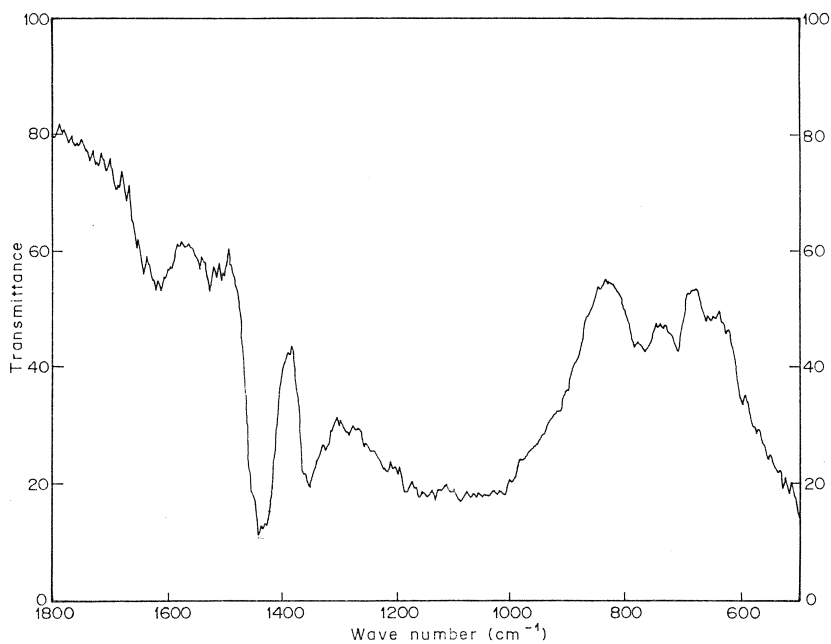
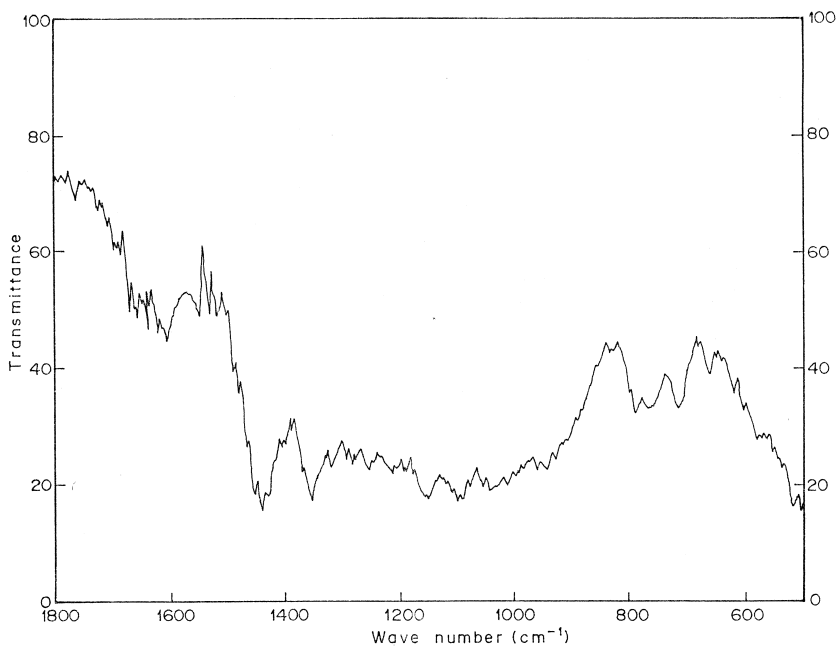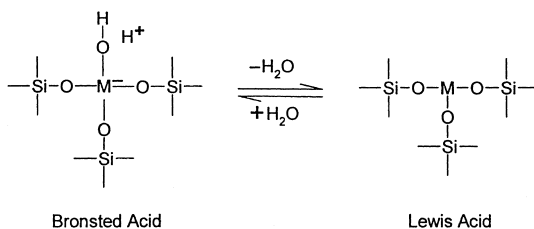Fig. 8. IR spectra of cyclohexylamine adsorbed in acid activated A3 sample.

Fig. 9. IR spectra of cyclohexylamine adsorbed in acid activated A4 sample.

general isomorphous substitution of M for Si^{4+} in the tetrahedral manifold of the montmorillonite leads to Lewis acidity. The equilibria between Bronsted and Lewis acid sites can be represented as follows:

Bronsted Acid   **Lewis Acid**

Further characterization of changes in the Bronsted sites on acid activation was studied from the infrared spectra of cyclohexylamine adsorbed on the clay montmorillonite (see Figs. 6–9). Peaks associated with Bronsted activity are observed at ≈ 1510 cm^{-1} i.e., indicating the presence of $-NH_3^+$. The $-NH_2$ was expected between 1600 and 1650 cm^{-1}, but this has been diminished by OH deformation resulting from water in the interlamellar layer.

3.3. Electrodeposition of polyaniline on acidified clay modified electrode

The working electrode was modified using acidified clay samples A1, A2, A3 and A4. The preparation of the electrode was achieved in the same manner as described in a previous work involving raw bentonite [26]. The resultant electrodes were stable and gave reproducible electrochemical data even after staying for a period of seven days. The polyaniline film was obtained by cycling the potential of the modified electrode in an electrolyte media containing 0.1 M aniline and 1 M sulphuric acid from -0.2 to 0.80 V at a scan rate of 20 mV/s. The resultant cyclic voltammograms had very sharp, clearly defined redox peaks as compared to the bare electrode or raw bentonite (unacidified) modified electrode case (see Fig. 10). This observation was true for all the acidified electrodes.
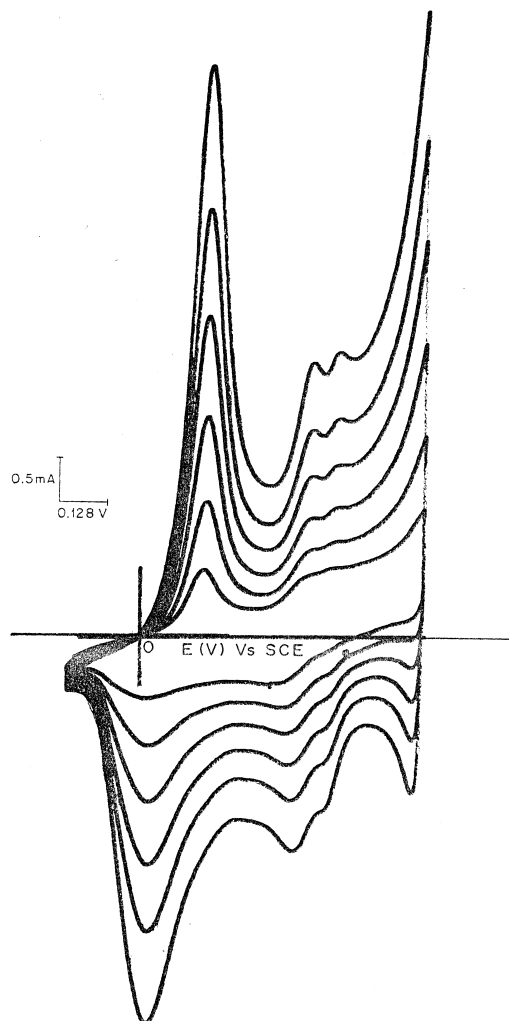
The oxidation potential occurred at $+0.165$

Fig. 10. Cyclic voltammogram of A2 modified carbon graphite electrode on cycling the potential in the range -0.2 to 0.8 V at a scan rate of 20 mV/s in a solution containing 0.1 M aniline and 1 M sulphuric acid.

Table 2
Effect of pH on polyaniline oxidation potential

Concentration sulphuric acid (M)	$E_{p,a}$ (V)
0.1	0.158
0.5	0.168
1.0	0.181
1.5	0.190
2.0	0.210

V, representing a shift towards negative potentials of ≈ 16 mV as compared to the bare electrode case. Thus, in this case the polymer is a lot easier to oxidize. This observation is rather intriguing in the sense that, the acidified clay which is supposedly a low pH matrix (as a result of the acidification) should have resulted in a positive shift in polyaniline redox potential as normally observed in the case of polyaniline electrodeposited on a bare carbon electrode (see Table 2). This implies that the actual pH in the host matrix is higher than expected and/or the protons on the acidified clay are not accessible to the polymer.
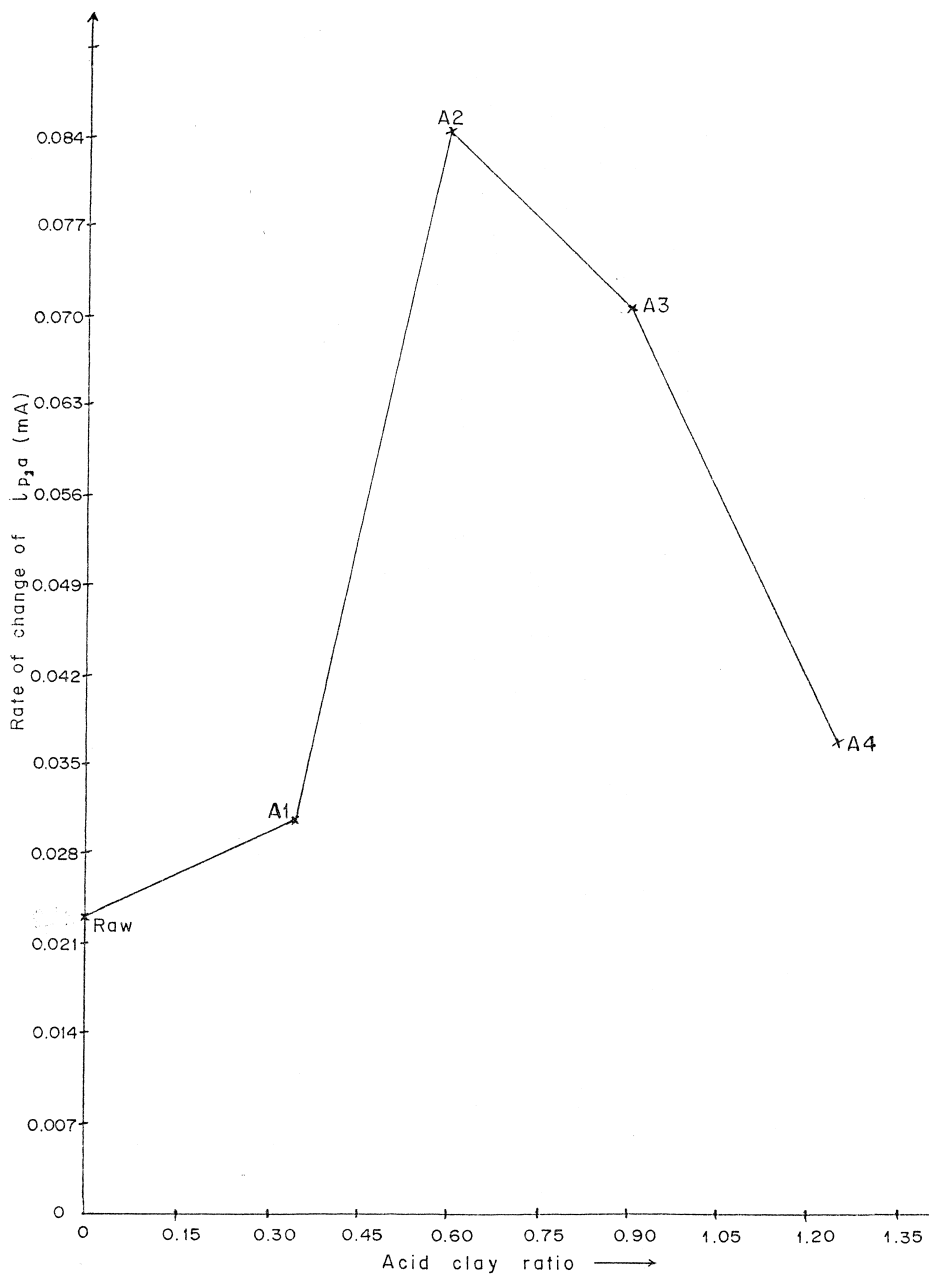

Fig. 11. Plot of rate of change of anodic peak current $I_{p,a}$ (mA) versus the acid-to-clay ratio.

This result suggest that the protons in the clay montmorrilonite are not just loosely held at the surface, thus are in no position to ingress into the polyaniline matrix as would be the case for an external acid solution.

We further observed that the peaks normally attributed to quinone/imine derivatives [2] in the case of polyaniline electrodeposited on acidified electrode are more pronounced than on bare carbon electrode case. The double humped oxidation peak occur at ≈ 0.418 and 0.473 V, respectively. In the bare electrode case it appears as a shoulder at ≈ 0.352 V.

It is also important to mention that the intensity of the peak at 0.418 V increases markedly as we increase the potential limit. This behaviour is also characteristic of polyaniline electrodeposited on a bare carbon electrode. Another feature of polyaniline on acidified clay electrode is enhanced switching rate as can be seen in Fig. 10 i.e., variation of the anodic peak current versus the potential at the onset of oxidation.

Another significant observation was the difference in the electrodeposition rate of polyaniline on the various modified electrodes (see Fig. 11). We observe low electrodeposition rate for electrode modified with raw and A1 bentonite, the highest electrodeposition rate being registered for the A2 modified electrode. The electrodeposition rate drops for the higher acid-to-clay ratios, i.e., A3 and A4.

Based on the data in Fig. 11, we propose that we obtain the same material but at different rates. The difference in the rates are resulting from the differences in metal cation and/or proton population in the electrode modification material.

4. Conclusion

The results presented in this paper indicate that the redox properties of polyaniline can be altered significantly by changing the population of Lewis and Bronsted acid sites in the clay montmorillonite used to derivatize the electrode surface.

References

[1] R. De Surville, M. Jozefowicz, L.T. Yu, J. Perichon, R. Buvet, Electrochim. Acta 13 (1968) 1451.

[2] E.W. Paul, A.J. Ricco, M.S. Wrighton, J. Phys. Chem. 89 (1985) 1441.

[3] A.G. MacDiarmid, J.C. Chiang, M. Haipern, W.S. Huang, S.L. Mu, N.L.D. Somasiri, W. Wu, S.I. Yaniger, Mol. Cryst. 121 (1985) 173.

[4] A.F. Diaz, J.A. Logan, J. Electroanal. Chem. 111 (1980) 111.

[5] T. Kobayashi, H. Yoneyama, H. Tamura, J. Electroanal. Chem. 161 (1984) 419.

[6] D. Orata, D.A. Buttry, J. Am. Chem. Soc. 109 (1987) 3574.

[7] X.L. Wei, Y.Z. Wang, S.M. Long, C. Bobeezko, A.J. Epstein, J. Am. Chem. Soc. 118 (1996) 2545.

[8] H. Yoneyama, H. Tamura, T. Kobayashi, J. Electroanal. Chem. 177 (1984) 291.

[9] G. Villemure, A.J. Bard, J. Electroanal. Chem. 282 (1990) 107, and references therein.

[10] C.N. Rhodes, D.R. Brown, J. Chem. Soc. Faraday Trans. 88 (1992) 2269.

[11] C.N. Rhodes, D.R. Brown, J. Chem. Soc. Faraday Trans. 89 (1993) 1387.

[12] C. Pesguera, F. Gozalex, I. Bentino, C. Blanco, S. Mendioroz, J. Pajeras, J. Mater. Chem. 2 (1992) 907.

[13] S. Mendioroz, J. Pajeras, I. Bentico, C. Pesquera, F. Gozalex, C. Blanco, Langmuir 3 (1987) 676.

[14] M.K.H. Siddiqui, in: Bleaching Earths, Pergamon Press, London, 1968, p. 33, Ch. 5.

[15] D.A. Morgan, D.B. Shaw, M.J. Sidebottom, T.C. Soon, R.S. Taylor, J. Am. Oil Chem. Soc. 62 (1984) 292.

[16] S.S. Cady, T.J. Pinnavaia, Inorganic Chem. 17 (1978) 1501.

[17] H. Van Damme, M. Crespin, F. Obrecht, M.I. Cruz, J.J. Fripiat, J. Colloid Interface Sci. 66 (1978) 43.

[18] P. Canesson, M.I. Cruz, H. Van Damme, in: M.M. Mortland, V.C. Farmer (Eds.), International Clay Conference, 1978, p. 217.

[19] S. Abdo, M.I. Cruz, J.J. Fripiat, Clays Clay Min. 28 (1980) 125.

[20] F. Bergaya, H. Van Damme, Geochim. Cosmochim. Acta 46 (1982) 349.

[21] P.K. Ghosh, A.J. Bard, J. Am. Chem. Soc. 105 (1983) 5691.

[22] P.K. Ghosh, A.W.H. Mau, A.J. Bard, J. Electronal. Chem. 169 (1984) 315.

[23] E.D. Ege, P.K. Ghosh, J.R. White, J.F. Equey, A.J. Bard, J. Am. Chem. Soc. 107 (1985) 5652.

[24] R. Mokaya, W. Jones, in: Ion-Exchange Processes: Advances and Applications, 1992, pp. 244–252.

[25] J. Fijal, Z. Klepyta, J. Zietkiewicz, M. Zyla, Mineral Pol. 6 (1975) 29.

[26] D. Orata, B. Kariuki, React. Funct. Polymers 28 (1996) 287.